

Dimensional effects on failure of concrete loaded in Mode II and III

G. Ferro, B. Chiaia & F. Gianola

Dept. of Structural Engineering and Geotechnics, Politecnico di Torino, Torino, Italy

ABSTRACT: Concrete collapse is seldom governed by crack propagation in pure Mode I (*opening*), due to loading and geometrical complexities. Usually, a superposition of the three modes of propagation occurs. In the laboratory, instead, the tests are normally performed by loading structures in Mode I. Moreover, such tests are conducted on smaller samples with respect to the real dimension. These two factors should be analyzed in order to get the actual strength and toughness for real structural members.

The Authors proposed the so-called Multifractal Scaling Law, largely validated in presence of failure in pure Mode I and especially in absence of large pre-notches. In the present work, the MFSL is applied to failures in Mode II (*sliding*) and Mode III (*tearing*). The interpretation of experimental tests for shear and torsion permits to affirm that the interaction between the microstructural characteristic length and the external structural size governs the scale effects also in Mode II and III.

1 INTRODUCTION

Fracture propagation in concrete and mortar has been generally analyzed when the crack advances orthogonally to the maximum principle stress, in pure Mode I (*opening mode*). Effectively, in concrete structures we have always experimentally observed fracture propagation in Mode I, even in presence of bi- and tri-axial state of stress, as in the collapse of large beams and plates, in the collapse for tear and for punching. Consequently, the strength and toughness parameters definition for collapse in Mode II and III is often considered useless.

It is opportune however to distinguish between *crack initiation* and *limit state*. This is essential nowadays as semi-probabilistic approaches for design at limit state split the two aspects and tend to assure structural integrity with respect to catastrophic collapse. In fact, crack initiation of the single microcrack is always governed by local tension stress (Mode I) generated by singularities due to microstructural heterogeneities and to pre-existent defects, while meso- and macro-phase of propagation impose the interaction of *in-plane shear or sliding* (Mode II) and *antiplane shear or tearing* (Mode III).

Fracture propagation in Mode II and III has been observed, for concrete, in all dynamic shear test, during impact resistance and in bullet penetration tests. In all these cases, a generalized fracture toughness has been determined, and it has been obtained that $G_{II} > G_{III} > G_I$.

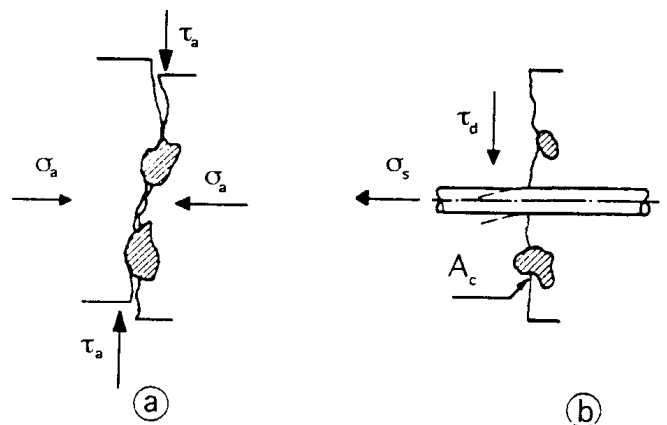


Figure 1. Mechanisms of transmission for shear forces in ultimate limit state.

When the microstructural roughness is involved in propagation resistance mechanisms, it is necessary to define correct mechanics parameters for Mode II and III. This is what happens for shear and tearing ultimate limit state, for seismic loads and for all structures cracked under loads in general. It is commonly considered that in these conditions, crack propagation in Mode I is localized and discontinuous, limited to very small scales, while Mode II and III dominate in collapse phase, characterized by continuous fracture. This phenomenon is evident in twist test on notched specimen by (Bažant et al., 1988), where Elastic Theory provides a stress and strain field, antisymmetric with respect to final fracture surface. As the fracture

surfaces are plane and normal to applied twist moment, they represent Mode III fractures. The micro-structural interlocking appears very important in tear collapse, the warping being not permitted.

The present Codes are generally calibrated to give an adequate safety parameter with respect to crack initiation for shear-twist. Unfortunately, crack initiation load is generally not proportional to collapse load. This can be, in fact, much less or only lightly less than ultimate load, by varying size of the considered element and other factors (micro-structure, load rate, etc.). Consequently, a correction from classical formulae is necessary, in order to maintain a homogeneous safety margin with respect to shear brittle collapse by varying structural size.

The present Italian Code (DM, 1996), in accordance with Eurocode 2 (EC2, 1995), considers both the aggregate interlocking (Fig. 1.a), which increases the resistance shear load for beams with a depth $d \leq 0.60\text{m}$, and the so called Dowel action, which represents the load capacity of a longitudinal steel reinforcement in the normal direction with respect to its axis (Fig. 1.b). This Code (DM, 1996) establishes to calculate the **resistance shear load** at ultimate limit state V_{sdu} as following:

$$V_{sdu} \leq 0,25f_{ctd}r(1 + 50\rho_l)b_wd\delta, \quad (1)$$

in which f_{ctd} is the tensile strength; $r = (1.6 - d)$, with d (section depth) expressed in meters and $d \leq 0.60\text{ m}$; $\rho_l = A_{sl}/(b_wd)$: this coefficient takes into account A_{sl} , which is the longitudinal reinforcement area; b_w is the shear resisting section width; δ is a dimensionless coefficient depending on load conditions. Eurocode 2 (EC2, 1995) similarly establishes to calculate the shearing strength V_{Rd1} as following:

$$V_{Rd1} = [\tau_{Rd}k(1,2 + 40\rho_1) + |0,15|\sigma_{cp}]b_wd, \quad (2)$$

in which $\tau_{Rd} = (0,25 f_{ctk0,05})/\gamma_c$ is the unitary shearing strength, γ_c being a dimensionless coefficient; $k = (1.6 - d)$; $\sigma_{cp} = N_{Sd}/A_c$, N_{Sd} being the longitudinal force in the section, due to loads or to pre-compression. These two formulas are very similar, because both take into account the contribution of the aggregates as well as of steel reinforcements. While in the Italian Code though V_{sdu} is proportional to the coefficient $(1 + 50\rho_l)$, in the Eurocode V_{Rd1} is proportional to the coefficient only if $\sigma_{cp} = 0$.

These approaches seem inadequate. They are empiric and do not take into account the micro-structural characteristic of concrete.

According to ACI Building Code (ACI-318-89, 1989), the basic expression for Shear Strength V_C of members subject to shear and flexure without shear reinforcement is the following:

$$V_C = \left(1.9\sqrt{f'_c} + 2500\rho_w \frac{V_u d}{M_u} \right) b_w d, \quad (3)$$

in which the three variables ($\sqrt{f'_c}$ is a measure of concrete tensile strength, ρ_w and $V_u d/M_u$, where V_u and M_u are the factored shear and moment occurring at section considered) affect shear strength. Some research data (Kani, 1967) has indicated that in eq.3 shear strength decreases as the overall depth of member increases.

2 SIZE-EFFECT LAW FOR STRENGTH IN MODE II AND III

Dimensional scale-effects emerge in many aspects of the so-called disordered materials mechanical behavior. The primary cause of these dimensional effects is represented by the heterogeneity of the material, which is the origin of local cracks in Mode I as well. The existence of an internal length which interacts with the external dimension of the considered specimen is the consequence. The collapse due to brittle propagation of a crack in Mode II or III clearly shows the peculiar features of critical phenomena, characterized by hierarchical evolution of micro-cracks, starting from the initial casual distribution of defects to the coalescence of micro-cracks in the final crack surface. The progressive transition from local Mode I to global Modes II and III shows as well the typical cuspidal (catastrophic) type instabilities.

The self-similar and hierarchical evolution of the damage has been extensively verified by experimental tests (Carpinteri et al., 1995). The multi-scale propagation in Modes II and III reflects the hierarchical character of concrete microstructure, which ranges from the microscopical scales of clinker to the mesoscales of aggregates, embedded in the concrete matrix. Fractal Geometry allows to abandon the integer dimensions of the euclidean sets and to synthetically describe, by means of non-integer topological dimensions, the heterogeneous and self-similar domains inside the concrete. In this way it is possible to quantify the degree of disorder of the material microstructure and to deduce the structural effects of the microscopic complexity. Due to the chaotic evolution of the damage in the material, the assumption of a *lacunar* (rarefied fractal of dimension less than 2) reacting section is however more adherent to reality than the classical assumption of an euclidean smooth and compact area (dimension = 2). It is consequently necessary to consider a topological dimension Δ_τ less than 2 ($[L]^{2-d_\tau}$), where d_τ represents the dimensional decrement due to the chaotic damage to all scales. In this manner it is possible to draw an elegant and synthetic description of the strain field when varying the observing scale, and, by means of a renor-

malization procedure (Carpinteri, 1994), the stress τ^* ($[F][L]^{-(2-d_\tau)}$) is obtained; this parameter is anomalous but independent from the scale. This invariant quantity allows to easily deduce the dimensional dependence of the nominal strength parameter τ_N (defined on the ideal *ligament* as $[F][L]^{-2}$), which is controlled by the fractal dimensional decrement d_τ .

Applying such ideas to structural level, the nominal shear strength decreases with considered element height increasing; this variation is controlled by the fractal dimension Δ_τ (and hence by the damage entity) of the resisting section. On the other side, as the structural dimension increases, considered stress fields progressively homogenize. Taking into account the limits of microscopes scales, the fractal dimension cannot be lower than 1.5; this confirms that fracture propagation process is a dissipative (Brownian) phenomenon. Small structures will take more benefit of the propagation process fractal character. On the other side in larger structures fractality disappears at a structural level (even if it still controls the phenomenon at a local level), and typical euclidean descriptions give acceptable results. Dimensional scale effect is very strong on small beams, in which the disorder influence is remarkable, while it smoothes down with external dimensions increasing. This transition from disorder to order (*geometrical multifractality*) is controlled by the interaction between the characteristic microstructural length (which can be expressed by an internal length l_{ch}) and external dimensions.

The multifractal approach fully agrees with the classic Cohesive Model (Hillerborg et al., 1976); this model considers the ratio between the characteristic dimension of the process zone (in which energetic dissipations take place) and the beam dimension as a marker of the influence of material microstructural disorder on material strength. On the other side, this approach is revolutionary with respect to Bažant Scale Energy Law (SEL) (Bažant, 1984), since the scale effect rate has an opposite trend.

On the basis of these arguments, a simple equation which allows to model the scale effect on tensile strength σ_N (Mode I), has been obtained, and it is largely supported by available data (Carpinteri et al., 1995). Such relationship can be extended to Mode II and III failure cases, simply introducing a nominal shear strength parameter τ_N instead of normal tensile stress σ_N . Applying the renormalizing procedure and considering the euclidean fractal transition, the analytical expression of MultiFractal Scale Law (MFSL) can be written as:

$$\tau_N = \tau_\infty \left(1 + \frac{l_{ch}}{d} \right)^{\frac{1}{2}} \quad (4)$$

where l_{ch} represents the internal length that sets the limit between fractal behavior, in which disorder pre-

vails and scale effect is strongly present, and euclidean behavior, where the disorder effect disappears and a constant asymptotic value of shear resistance τ_∞ is reached. It needs to be noticed that the scaling curve slope is ruled by the ratio between l_{ch} and the referring structure dimension d , and that the Brownian hypothesis gives the exponent 1/2, which has the same value as the curve slope (maximum scale effect) for very small structures. In the bilogarithmic diagram (fig 2), MFSL shows a concave behavior, where SEL shows a convex behavior (Bažant, 1984).

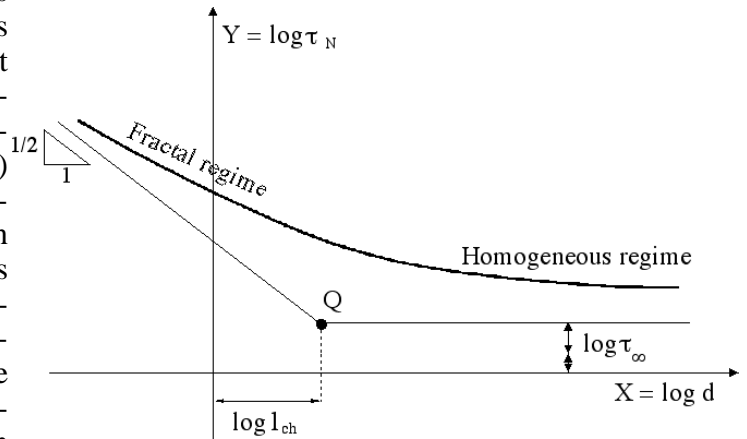


Figure 2. Multifractal Scale Law for ultimate shear stress.

From an engineering point of view, eq. 4 allows to determine the shear strength (or the torsional strength) on very large structures, while the SEL forecasts null resistance on larger scales. Furthermore, the internal length parameter, which is function of concrete microstructural characteristics, allows to make a distinction among various concrete mixtures and to identify, case by case, the minimum dimension exceeding which classic euclidean model can be used. A great number of tests, as shown in the following paragraphs, confirms the validity of MFSL in cases of collapse due to propagation in Mode II and III. The dispersion of experimental strength values decreases with specimen dimension increasing, showing the essential influence of heterogeneity.

3 APPLICATION OF MFSL TO EXPERIMENTAL DATA IN MODE II

Experimental tests in which concrete specimens are subject to a pure Mode II state of stress are analysed in this paragraph. It is important to notice that from an experimental point of view, creating a load system which generates a pure Mode II state of stress is very difficult, therefore the knowledge of such collapse is still quite limited and related results are very few. The *four point shear specimen* (Fig.3), proposed for the first time by Iosipescu (Iosipescu, 1967), is the mostly used shearing test model and it has been further devel-

oped in many versions. Such double-notched geometry presents a state of stress which is associable to a mixed Mode, where Mode II is clearly prevalent over Mode I.

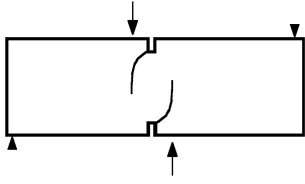


Figure 3. Shearing test chart according to Iosipescu (Iosipescu, 1967).

A number of shearing tests were performed at Politecnico di Torino (Bocca et al., 1990), using the classic *four point shear specimen* geometry. Specimen width was kept constant and equal to $b=100$ mm, with a ratio span-height l/d of 4, and with $d=50, 100, 200$ mm for the three different tested dimensions. Therefore the reached scale range was equal to **1:4**. The concrete had a water-cement ratio of 0.5, with maximum aggregate dimension $d_{max}=10$ mm. Compressive strength, measured on 160 mm side cubes, resulted equal to 33.7 MPa. A displacement-control machine (with maximum load of 100 kN) was used to apply the load. A constant increase of the slip between the two crack faces of 2.5×10^{-8} m/s, measured by a DD1 transducer, was taken as a control parameter. Three sets of tests were made, varying the arm between the two central forces: in the first set the ratio between arm c and height d was 0.4, in the second one the ratio c/d is 0.8 and in the third one the ratio was 1.2. The ratio between notch-length and beam-height was set 1:2 in all tests. In order to determine maximum nominal shear stress the following conventional formula was used:

$$\tau_N = \frac{P_{max}}{bd} \quad (5)$$

where b and d are specimen base and height respectively, while P_{max} represents the maximum load reached during the test.

The application (Fig. 4) of Multifractal Scale Law in tests where $c/d=0.4$ led to the following parameters: $\tau_{\infty}=1.49$ MPa and $l_{ch} = 77.7$ mm, while with $c/d=0.8$ it led to: $\tau_{\infty}=1.41$ MPa and $l_{ch} = 99.2$ mm. Correlation coefficient R showed that MFSL gives a better data interpretation than SEL (Fig. 4). Dimensionless ratio l_{ch}/d_{max} gave the dimensionless quantity α of 7.77 in the first case and 9.92 in the second one.

Parallel Mode II tests, made on a similar geometry, were realized by (Bažant and Pfeiffer, 1987). These

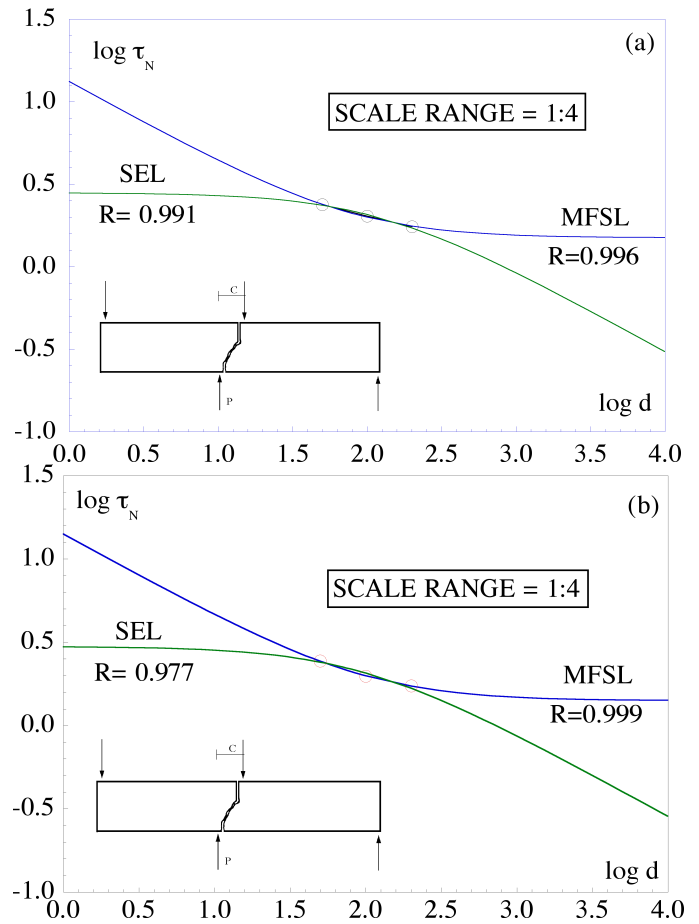


Figure 4. Application of Multifractal Scale Law to shearing tests (Bocca et al., 1990): (a) $c=0.4$; (b) $c=0.8$.

tests were made both on concretes and mortars. Specimens, which had a prismatic shape, showed a rectangular section and a ratio length-width of 8/3. Height d assumed the following values: 38.1, 72.2, 152.4 and 308.8 mm. Width was kept constant and equal to 38.1 mm. Each specimen had two notches in the middle, $d/6$ in length and 2.5 mm wide. Concrete used in the tests was characterized by a cement-fine aggregate-coarse aggregate ratio, expressed in weight, of 1:2:2 and by a water-cement ratio of 3:5. The maximum size of coarse aggregate, which consisted of calcareous rocks, was $d_{max}=12.7$ mm, while light aggregate maximum size was equal to 4.8 mm. Mortar was characterized by a cement-fine aggregate ratio of 1:2 and by a water-cement ratio of 1:2. Cement and sand used to prepare the concrete were the same ones used to prepare the mortar, therefore the maximum aggregate dimension is 4.8 mm. Compressive strength, measured on cylindrical specimens (diameter of 76 mm and height of 152.4 mm), resulted 37.9 MPa for concrete and 49 MPa for mortar. A displacement-control machine was used, with maximum load of 100 kN. The specimen was loaded by four vertical forces: three of them were transmitted by rollers, one by a hinge, in order to guarantee the equilibrium in the hor-

horizontal direction.

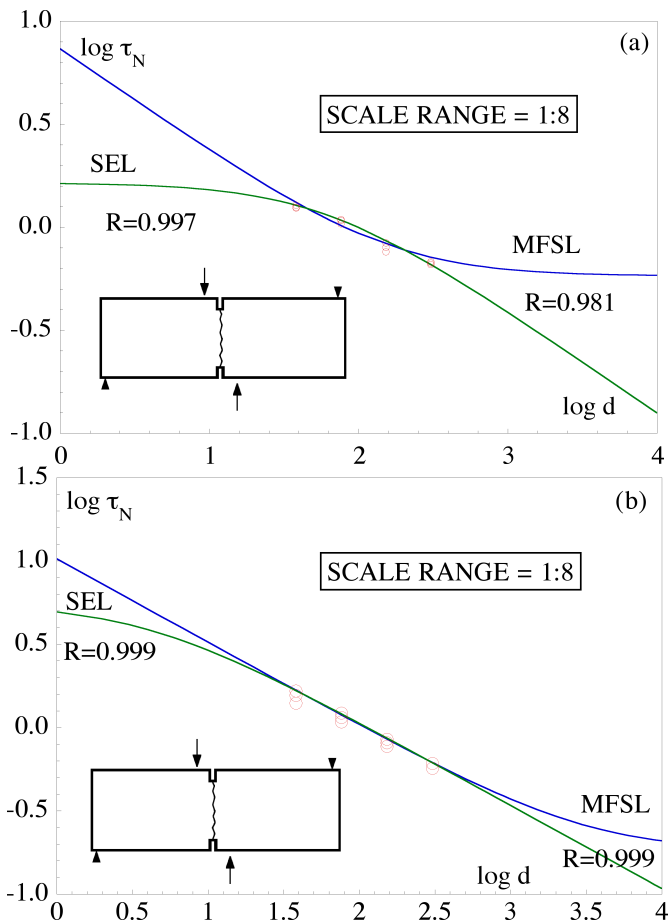


Figure 5. Application of MFSL to (Bažant and Pfeiffer, 1987) experimental results, with a distance between central forces of d : (a) concrete, (b) mortar.

Two sets of tests were performed for each conglomerate, varying the distance between the two central forces: in the first set the distance was $1/12 d$ and d in the second one. According to the authors, the second test was necessary to verify the odd trend of the crack which connected one notch to the other: this crack apparently violated classic criteria of crack propagation. They affirmed that the crack vertical development represented a propagation in pure Mode II, but this was denied by Schlangen (Schlangen, 1993). He repeated the same tests, and pointed out how actually the authors were controlling forces and not displacements, therefore obtaining a brittle crack propagation.

Application of Multifractal Scale Law to the I set of tests on concrete (Fig. 5.a) led to the following two parameters: $\tau_\infty=0.58$ MPa and $l_{ch} = 159.8$ mm, while for mortar (Fig. 5.b) to: $\tau_\infty=0.18$ MPa and $l_{ch} = 3181$ mm. Correlation coefficient R was equal to 0.981 according to MFSL and to 0.997 according to SEL in the case of tests on concrete, while it was equal to 0.999 according to both Laws in the case of mortars. Dimensionless ratio l_{ch}/d_{max} gave the dimensionless quantity α equal to 12.6 for concrete and 662 for mor-

tar.

4 APPLICATION OF MFSL TO EXPERIMENTAL DATA IN MODE III

Prescriptions in force (EC2, 1995) about simple and reinforced concrete structures torsional collapse are based on Plastic Limit Analysis exclusively. As a consequence no dimensional effect is taken into account, unlike shear collapse, in which at least gear effect, due to superficial roughness, is measured by calculus standards.

Nevertheless, torsional collapse appears to be clearly brittle and not ductile, as observed in tests; these showed that load does not reach a horizontal *plateau* but decreases rapidly after having assumed the peak load value. Furthermore, brittleness increases with element size, which means that larger beams collapse immediately after the peak load value, without showing any *softening* and almost explosively. Therefore the conclusion can be that structural dimensions have a great influence on ultimate strength and ductility in torsional collapse.

The need to determine strength variation for torsion ultimate limit state seems to be even stronger, if it is taken into account that ultimate load, measured in longitudinally reinforced concrete beams, is smaller than ultimate load measured in not reinforced beams with the same dimensions.

Geometries which were tested to study the scale effect on ultimate torsion strength aimed to generate a stress state as much antisymmetric as possible, with respect to the beam section, in order to originate a macroscopic propagation of pure Mode III.

The first set of tests in Mode III which is going to be exposed was performed by (Bažant et al., 1988) and it was carried out on micro-concretes, reinforced and not. Analysed specimens had a prismatic section, with side d and length L . Three different dimensions of d , were used, 38.1, 76.2 and 152.4 mm respectively; ratio $L/d=8/3$ was kept constant for all beams. Beams were torsionally loaded by two opposite pairs on the two extreme sections. Load pair arms were taken equal to 19.1, 38.2 and 127 mm respectively. Pair forces were applied at a distance a from the extreme sections; ratio $a/L=3/32$ was constant for all beams. Specimen maximum aggregate dimension d_{max} was 4.8 mm. The water-cement-fine aggregate-coarse aggregate weight proportions employed stood in the ratio 0.6:1:2:2. Compressive strength tests were made on cylindrical specimens obtained from the beams cast; these specimens gave a strength value of 43.6÷44.1 MPa.

In reinforced specimens bars were placed in correspondence of transversal section vertices, with an internal arm of 8.1, 16.3, 31.5 mm and with a diameter of 3.18, 6.35 and 12.7 mm respectively. For smaller

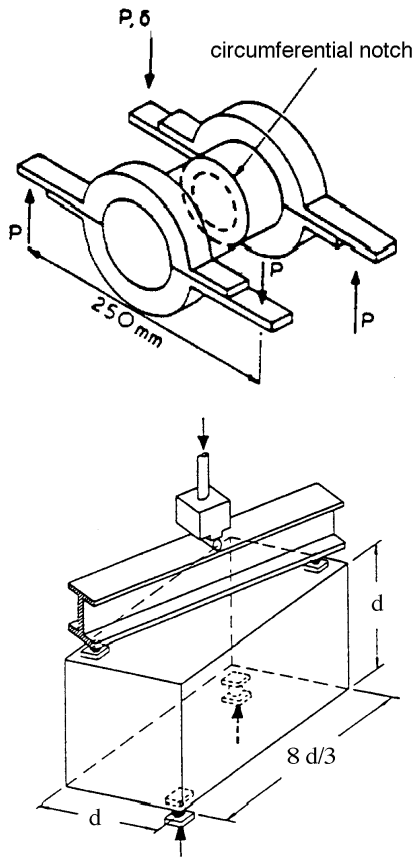


Figure 6. Torsion tests charts according to (Tokatly and Barr, 1991) (Bažant and Pfeiffer, 1987).

diameters yield strength f_y resulted equal to 310 MPa, while for bigger to 413 MPa. In accordance with Elasticity Theory, maximum shear stress can be expressed as:

$$\tau_N = 4.80 \frac{M_z}{d^3}, \quad (6)$$

where M_z is the maximum twisting moment. MFSL parameters for not reinforced beams τ_∞ and l_{ch} resulted to be equal to 1.72 MPa and 148.0 mm respectively, while ratio l_{ch}/d_{max} is equal to 30.84. *fitting* according to MFSL (Fig. 7.a) gave a correlation coefficient of 0.977, while according to SEL a value of $R=0.994$, dimensional of experimental data, was obtained. For reinforced beams (Fig. 7.b) values obtained are: $\tau_\infty=1.367$ MPa, $l_{ch}=246.6$ mm and $l_{ch}/d_{max}=55.11$. It can be noticed in Fig.7 that the two Laws show approximately the same linear trend in the tested dimensional gap, in which a monofractal *scaling* is present.

The second kind of torsion test was performed by (Barr and Tokatly, 1991; Tokatly and Barr, 1991), and it was carried out on both notched and un-notched cylindrical concrete specimens. Four different diameters were tested (80, 100, 150 and 200 mm); specimen length was taken as twice the diameter in each

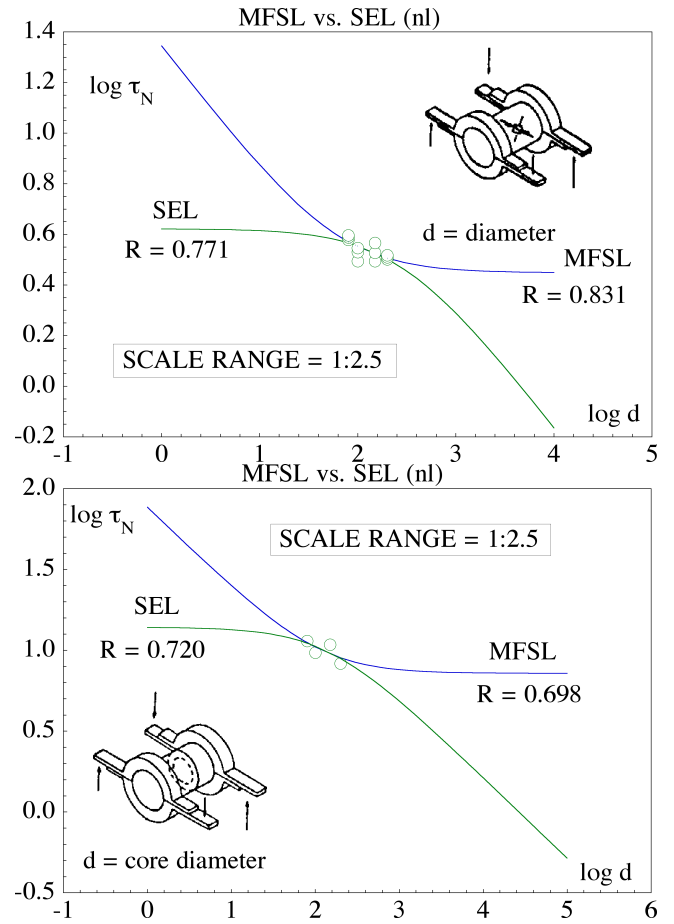


Figure 7. Application of MFSL to experimental results of (Bažant et al., 1988): not reinforced micro-concrete (a), reinforced microconcrete (b).

case. The dimensions of the specimens varied within the range 1:2,5, which is quite limited. Concrete had a cement : light aggregate : coarse aggregate ratio of 1:1.8:2.8. Water : cement ratio was equal to 0.5, which gave origin to a compressive strength of 50-55 MPa. Maximum aggregate diameter was $d_{max} = 10$ mm. Notch length in notched specimens was taken equal to $d/5$, where d represented the specimen diameter. In accordance with Elasticity Theory, maximum shear stress can be calculated by the following formula:

$$\tau_N = \frac{16M_z}{\pi d^3} \times 10, \quad (7)$$

where M_z is the maximum twisting moment.

Applying MFSL to un-notched specimen results the following values were obtained: $\tau_\infty = 2.81$ MPa, $l_{ch} = 61.15$ mm and $l_{ch}/d_{max} = 6.11$, while applying it to notched specimens results the values were: $\tau_\infty = 5.75$ MPa, $l_{ch} = 209.96$ mm and $l_{ch}/d_{max} = 21.0$. Correlation coefficients for un-notched specimens were equal to 0.831 and 0.771 according to MFSL and SEL respectively, while for notched specimens the values $R(\text{MFSL})=0.920$ and $R(\text{SEL})=0.885$ were obtained. It can be inferred, through a graphic comparison of bilogarithmic diagram (Fig. 8), that in this case as

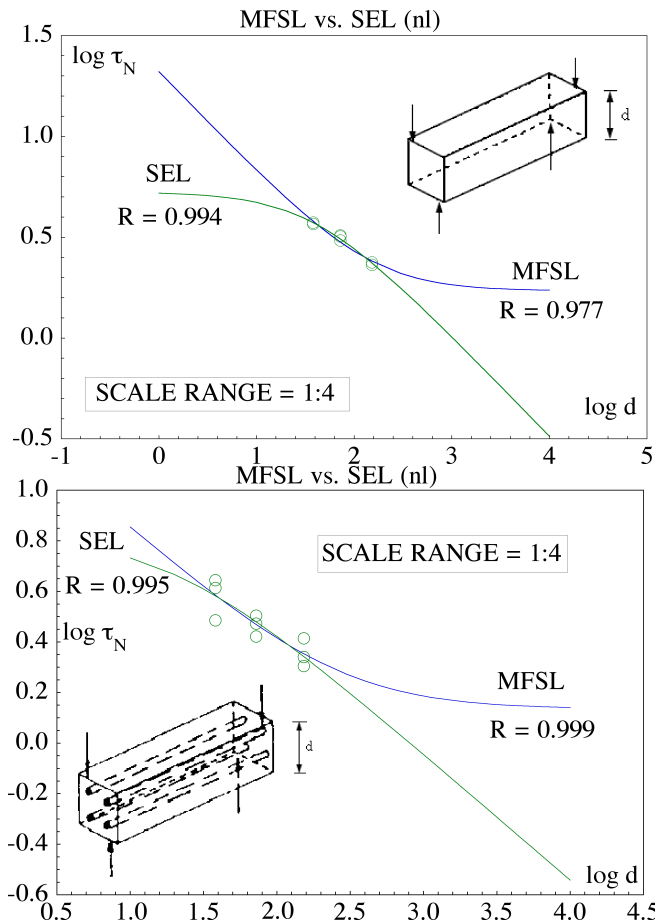


Figure 8. Application of MFSL to experimental results of (Barr and Tokatly, 1991; Tokatly and Barr, 1991): un-notched specimens (a), notched specimens (b).

well MFSL gives a better interpretation of experimental data than SEL.

5 CONCLUSIONS

Experimental tests for shear and torsion on concrete specimens subject to a pure Mode II or a pure Mode III state of stress show the validity of the Multifractal Scaling Law application in these cases. It is demonstrated in these tests that the interaction between the microstructural characteristic length and the external structural size governs the scale effects not only in Mode I but in Mode II and III as well. The MFSL allows to obtain significant constant values for strength and toughness for large structures, starting from the mechanical properties determined in the laboratory.

REFERENCES

ACI-318-89 (1989). Building code requirements for reinforced concrete. *ACI*.

Barr, B. and Tokatly, Z. Y. (1991). Size effects in two compact test specimen geometries. In Carpinteri, A., editor, *Applications of Fracture Mechanics to Reinforced Concrete*, pages 63–

93. Elsevier Applied Science.

Bažant, Z. P. (1984). Size effect in blunt fracture: concrete, rock, metal. *Journal of Engineering Mechanics, ASCE*, 110:518–535.

Bažant, Z. P. and Pfeiffer, P. (1987). Determination of fracture energy from size effect and brittleness number. *ACI Material Journal*, 84 (6):463–480.

Bažant, Z. P., Sener, S., and Prat, P. C. (1988). Size effects of torsional failure of plain and reinforced concrete beams. *Materials and Structures, RILEM*, 21:425–430.

Bocca, P., Carpinteri, A., and Valente, S. (1990). Size effect in mixed-mode crack propagation: softening and snap-back analysis. *Engineering Fracture Mechanics*, 35:159–170.

Carpinteri, A. (1994). Scaling laws and renormalization groups for strength and toughness of disordered materials. *International Journal of Solids and Structures*, 31:291–302.

Carpinteri, A., Chiaia, B., and Ferro, G. (1995). Size effects on nominal tensile strength of concrete structures: multifractality of material ligaments and dimensional transition from order to disorder. *Materials and Structures, RILEM*, 28:311–317.

DM (1996). Norme tecniche per il calcolo, l'esecuzione e il collaudo delle strutture in cemento armato normale e precompresso e per le strutture metalliche. *Gazzetta Ufficiale*, 29.

EC2 (1995). Commission of european communities. *Eurocode II: Design of Concrete Structures, Part I*.

Hillerborg, A., Modeer, M., and Petersson, P. E. (1976). Analysis of crack formation and crack growth in concrete by means of fracture mechanics and finite elements. *Cement and Concrete Research*, 6:773–782.

Iosipescu, N. (1967). New accurate procedure for single shear testing of metals. *Journal of Materials*, 2:537–566.

Kani, G. N. J. (1967). How safe are our large reinforced concrete beams. *ACI Journal*, 64:128–141.

Schlangen, E. (1993). Experimental and numerical analysis of fracture process in concrete. *Heron*, 38:1–117.

Tokatly, Z. Y. and Barr, B. (1991). Size effects in mode iii fracture. In van Mier, J. and Bakker, A., editors, *Fracture Processes in Concrete, Rock and Ceramics*, pages 473–482. E.& F.N. Spon.